CAV2021
11th International Symposium on Cavitation
May 10-13, 2021, Daejon, Korea

Dual-camera mode visualization of cavitating flows

James A. Venning[1]*, Bryce W. Pearce[1] and Paul A. Brandner[1]

[1]Cavitation Research Laboratory, University of Tasmania, Launceston, Tasmania, Australia

Abstract: The global mode visualization technique presented in Venning et al. [1] is extended to use two cameras, simultaneously recording a 3D cavitating flow from opposite directions. The cavitating flow investigated is that about a sphere at a transcritical Reynolds number of 1.5×10^6 and a cavitation number of 0.8. High-resolution data, in both time and space, allows detailed mode shapes to be obtained. The addition of the second camera significantly reduces the potential for ambiguity about the nature of the shedding modes and adds additional information in regions that would otherwise be obscured in a single-camera experiment. The global distribution of power and the phase for each cavity shedding mode are described, confirming a symmetric and asymmetric mode.

Keywords: modal decomposition; mode visualisation; cavitation; high-speed imaging; frequency analysis

1. Introduction

Modal decomposition methods have been used in a variety of fluid mechanics applications to approximately describe complicated physical phenomena with few dimensions. Two commonly used techniques are the proper orthogonal decomposition (POD) and the dynamic mode decomposition (DMD). The POD ranks spatial structures according to the kinetic energy for velocimetric data [2]. This allows filtering based on energy so that experimental noise and turbulence can be removed, highlighting the large-scale features in a flow. The DMD, on the other hand, is based on the growth-rates of frequencies, so that amplifying or decaying features can be extracted, but permanent features are not accentuated [e.g. 3, 4].

The technique used in this paper is based on the Fast Fourier Transform (FFT) of the pixel intensity in high-speed images. The objectives are to identify dominant frequencies in the videos, identify the regions in the spatial domain where these modes are manifested and to identify the phasing across the domain. This technique has been used previously in Basley et al. [5, 6] in cavity flows and [7] in wakes, and was extended to enable the 'averaging' of multiple time instances to remove noise from the modes by [8] for velocimetry data, or [1] for photographic data. This technique is equivalent to the spectral POD method as discussed in [9].

Here, we apply this technique to high-speed imaging acquired simultaneously from two cameras. While modal behaviour was discussed in [1], only one side of the flow could be imaged at that time, leaving some ambiguity about the true nature of the modes. In this study, the previous experiment has been repeated utilizing two cameras, each with quintuple the resolution and more than double the duration.

2. Experimental setup and data analysis

The flow was generated at the Cavitation Research Laboratory at the University of Tasmania. A 150 mm diameter PVC sphere was sting-mounted in the centre of the test section. The test-section velocity and pressure were controlled to hold the diameter-based Reynolds number at 1.5×10^6 and the cavitation number

* Corresponding Author: James Venning, james.venning@utas.edu.au

at 0.8, which corresponds to the energetic bi-modal shedding of large-scale cloud cavities [10]. Images were acquired with two symmetric high-speed Phantom v2640 cameras, capturing synchronized images of 5.2 megapixels at 9900 fps for 7.8 s. The cameras were mounted on each side of the tunnel test-section such that they were visualising the opposite sides of the sphere.

The 77.7×10^3 frames were decomposed using a Fourier transform with a Welch windowing methodology. The frequencies of interest were established from the average of all the spectra across the spatial domain, revealing two dominant frequencies. These correspond to the two modes identified from the pressure recordings of [10]. For each frequency, the complex array ($\boldsymbol{\Phi}_f$), which contains 72 temporal instances or Welch windows and 5,242,880 different spatial locations, was then factorized with the Singular Value Decomposition (SVD), recovering the typical mode shape from the eigenvectors of $\boldsymbol{\Phi}_f^T \boldsymbol{\Phi}_f$ and projecting them onto the basis eigenvectors: $\boldsymbol{\Phi}_f \boldsymbol{R}_f$, where $\boldsymbol{R}_f$ is the right-singular matrix from the SVD. A detailed description is given in [1]. As the first mode of each frequency is most representative of the flow, only this has been presented in the present study.

The modes are represented with a power, P, and a phase, Φ, which are the magnitude and angle of the complex variable $\boldsymbol{\Phi}_f \boldsymbol{R}_f$. The power represents how energetically that frequency is manifested at every location. The phase gives the angular difference of that frequency across the domain, relative to an arbitrary, but consistent, phase angle, and is presented by a cyclical colour map. Regions with constant phase are fluctuating at that frequency in-phase.

3. Results

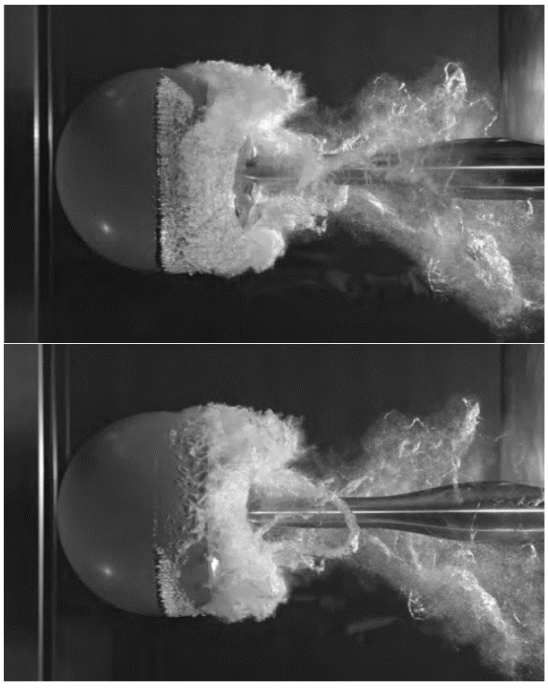

Figure 1. Simultaneous photographs from opposite sides of cloud cavitation about a sphere. The diameter-based Reynolds number is 1.5×10^6 and the cavitation number 0.8.

Simultaneous photographs from the two viewing directions (from opposite sides of the sphere) are given in Figure 1. This provides additional insight, particularly near the sphere body which only one side

* Corresponding Author: James Venning, james.venning@utas.edu.au

would usually be visible. In the wake, the same vortical cavitation structures can be observed on each side of the flow. This is particularly useful near the sphere body, where it is obvious that the cavity shedding cycle is at a different phase between the two sides.

The power (P) and phase (Φ) of the low-frequency mode (diameter-based Strouhal number, St, of 0.25) is presented in Figure 2. The power (in red) indicates that the fluctuations manifest both in the shear layers behind the sphere and on the body itself. The phase, Φ, in the lower plots show which regions of the intensity domain are in-phase. The solid contours are given to highlight some features, and indicate where the phase is near $\pm\pi/2$. The black contour in the lower left figure appears obliquely which indicates the presence of oblique clouds. The two images show the same phase and power information on both sides of the wake, as expected since the same clouds are being imaged. Behind the sphere and sting, only one camera can image each side, so the mode shape here would usually be unknown from a single camera. The phase in these regions are opposite, confirming the asymmetric nature.

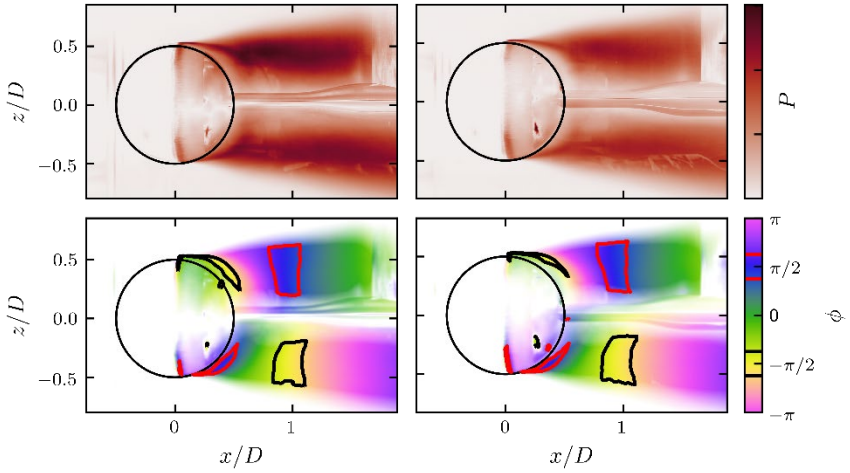

Figure 2. Distribution of the power (top) and phase (bottom) of the low-frequency mode ($St = 0.25$) for the two cameras. Areas of phase near $\pi/2$ and $-\pi/2$ are highlighted with the red and black contours, respectively. The mode is asymmetric

The power of the second, high-frequency, mode is concentrated mainly in the shear layer regions (Figure 3) and has a frequency of $St = 0.50$. The phase here is symmetric about the x direction, indicating the shedding of ring-like cavities. This is reminiscent of the vortex shedding of cavities at low Reynolds numbers [11].

Axisymmetric flow about the sphere drives nominally uniform cavity growth around the sphere circumference and nominally axisymmetric shedding of the cavitating vortex as a fundamental mode. Global instability leads to non-uniform cavity growth and subsequent asymmetric shedding of oblique vortices that in the wake are distorted to classical hairpin shaped vortices. The greater cavity lengths that develop in the asymmetric mode lead to greater shedding periods and hence this being the low mode. Given the nominal axisymmetry of the global flow it would be expected that the orientation of the shed hairpin vortices in the low mode will be random. In both modes the shedding mechanisms are the same driven by coupled re-entrant jet and shockwave phenomena [10].

4. Conclusions

Global modes from two synchronised high-speed cameras provide greater insights into the topology of cloud shedding about a sphere. Two modes are evident, a low-frequency, asymmetric mode of

* Corresponding Author: James Venning, james.venning@utas.edu.au

oblique vortices, and a higher-frequency, symmetric mode of ring vortices. Future work with distributed unsteady surface pressure sensing, simultaneous with dual high-speed cameras, should resolve remaining uncertainties of the global modes for a range of cavitation numbers.

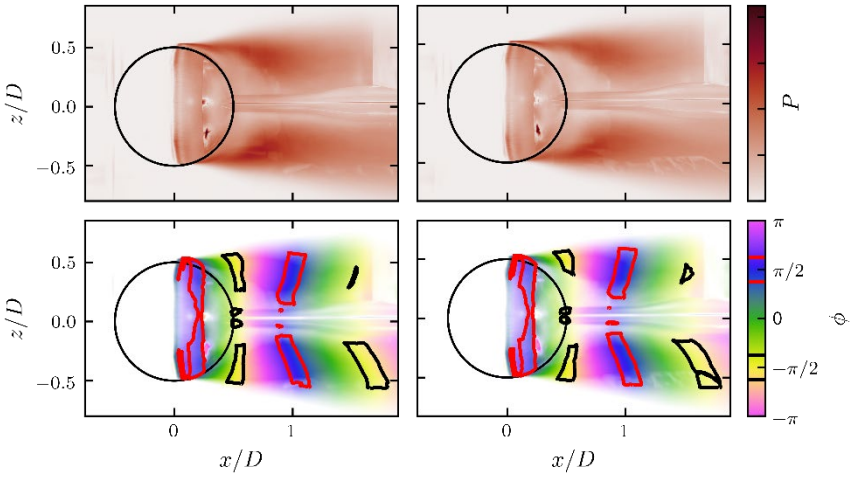

Figure 3. Distribution of the power (top) and phase (bottom) of the high-frequency mode ($St = 0.50$) for the two cameras. Areas of phase near $\pi/2$ and $-\pi/2$ are highlighted with the red and black contours, respectively. The mode is axisymmetric about the x-axis.

References

1. James A Venning, Dean R Giosio, Bryce W Pearce, and Paul A Brandner. Global Mode Visualization in Cavitating Flows. In *Proceedings of the 10th International Symposium on Cavitation* (CAV2018), pages 485–490. ASME Press, 2018.
2. Lawrence Sirovich. Turbulence and the dynamics of coherent structures. *Quarterly of Applied Mathematics*, 45(3):561–571, 1987. ISSN 0033-569X. doi: 10.1090/qam/910463.
3. Clarence W. Rowley, Igor Mezic, Shervin Bagheri, Philipp Schlatter, and Dan S. Henningson. Spectral analysis of nonlinear flows. *Journal of Fluid Mechanics*, 641:115, 2009. ISSN 0022-1120. doi: 10.1017/S0022112009992059.
4. Peter J. Schmid. Dynamic mode decomposition of numerical and experimental data. *Journal of Fluid Mechanics*, 656:5–28, 2010. ISSN 0022-1120. doi: 10.1017/S0022112010001217.
5. J. Basley, L. R. Pastur, F. Lusseyran, T. M. Faure, and N. Delprat. Experimental investigation of global structures in an incompressible cavity flow using time-resolved PIV. *Experiments in Fluids*, 50(4): 905–918, 2011. ISSN 07234864. doi: 10.1007/s00348-010-0942-9.
6. J. Basley, L. R. Pastur, N. Delprat, and F. Lusseyran. Space-time aspects of a three-dimensional multimodulated open cavity flow. *Physics of Fluids*, 25(6), 2013. ISSN 10706631. doi: 10.1063/1.4811692.
7. T. Mcqueen, J. Venning, and J. Sheridan. Effects of Aspect Ratio on the Wake Dynamics of the Ahmed Body. In *19th Australasian Fluid Mechanics Conference*, 2014. ISBN 9780646596952.
8. J Venning. *Vortex structures in the wakes of two- and three-dimensional bodies*. Phd, Monash University, 2016.
9. Aaron Towne, Oliver T. Schmidt, and Tim Colonius. Spectral proper orthogonal decomposition and its relationship to dynamic mode decomposition and resolvent analysis. *Journal of Fluid Mechanics*, 847:821–867, 2018. ISSN 14697645. doi: 10.1017/jfm.2018.283.
10. K. L. de Graaf, P. A. Brandner, and B. W. Pearce. Spectral content of cloud cavitation about a sphere. *Journal of Fluid Mechanics*, 812:R1, 2017. ISSN 0022-1120. doi: 10.1017/jfm.2016.819.
11. H Sakamoto and H Haniu. A Study on Wortex Shedding From Spheres in a Uniform Flow. *Transactions of the ASME*, 112(December):386–392, 1990.

* Corresponding Author: James Venning, james.venning@utas.edu.au